



Contents lists available at ScienceDirect

Journal of Organometallic Chemistry

journal homepage: www.elsevier.com/locate/jorganchem

Synthesis, crystal structures, and redox behavior of some pentamethylcyclopentadienyl arene ruthenium salts

Swagat K. Mohapatra^{a,b}, Alexander Romanov^c, Tatiana V. Timofeeva^c, Seth R. Marder^{a,*}, Stephen Barlow^{a,*}

^aSchool of Chemistry and Biochemistry and Center for Organic Photonics and Electronics, Georgia Institute of Technology, Atlanta, GA 30332-0400, USA

^bKIIT University, Bhubaneswar, Orissa 751024, India

^cDepartment of Chemistry, New Mexico Highlands University, Las Vegas, NM 87701, USA

ARTICLE INFO

Article history:

Received 18 March 2013

Received in revised form

9 July 2013

Accepted 9 July 2013

Keywords:

Ruthenium

Pentamethylcyclopentadienyl

Arene

Crystal structure

Redox potential

ABSTRACT

Hexafluorophosphates of (η^5 -pentamethylcyclopentadienyl)(η^6 -arene)ruthenium cations (arene = 1,3,5-triethylbenzene, 1,3,5-tris(trimethylsilylmethyl)benzene, and pentamethylbenzene) have been obtained from the reaction of $[\text{Ru}(\eta^5\text{-C}_5\text{Me}_5)(\text{NCCH}_3)_3]^+\text{PF}_6^-$ with the appropriate arene; their X-ray single-crystal structures have been determined and compared to those of related compounds. The electrochemistry of these cations is compared to that of other $[\text{Ru}(\eta^5\text{-C}_5\text{Me}_5)(\eta^6\text{-arene})]^+$ and $[\text{Fe}(\eta^5\text{-C}_5\text{Me}_5)(\eta^6\text{-arene})]^+$ species; the 1,3,5- $\text{C}_6\text{H}_3(\text{CH}_2\text{SiMe}_3)_3$ derivative is reduced at the most cathodic potential ($E_{\text{pc}} = -2.96$ V vs. ferrocenium/ferrocene). Reduction with sodium amalgam gives a dimer, $[\text{Ru}(\eta^5\text{-C}_5\text{Me}_5)]_2[\mu\text{-}\eta^5\text{:}\eta^5\text{-(arene)}_2]$, in the case of arene = 1,3,5- $\text{C}_6\text{H}_3\text{Et}_3$, analogous to what has been previously reported for the mesitylene complex, and a mixture of products when arene = C_6HMe_5 . The 1,3,5- $\text{C}_6\text{H}_3(\text{CH}_2\text{SiMe}_3)_3$ derivative is comparatively unreactive to sodium amalgam, although long reaction times lead to desilylation and formation of $[\text{Ru}(\eta^5\text{-C}_5\text{Me}_5)]_2[\mu\text{-}\eta^5\text{:}\eta^5\text{-C}_6\text{H}_3\text{Me}_3\text{C}_6\text{H}_3\text{Me}_3]$. Use of sodium–potassium alloy, on the other hand, leads to formation of a 18-electron anionic Ru⁰ complex: $\text{K}^+[\text{Ru}(\eta^5\text{-C}_5\text{Me}_5)\{\eta^4\text{-1,3,5-C}_6\text{H}_3(\text{CH}_2\text{SiMe}_3)_3\}]^-$.

© 2013 Elsevier B.V. All rights reserved.

1. Introduction

We have recently found that the “2 × 18-electron” dimers formed by certain 19-electron sandwich compounds, namely $[\text{RhCp}_2]_2$ [1,2], $[\text{FeCp}^*(\text{C}_6\text{H}_6)]_2$ ($\text{Cp}^* = \eta^5\text{-C}_5\text{Me}_5$) [3], and $[\text{RuCp}^*(1,3,5\text{-C}_6\text{H}_3\text{R}_3)]_2$ ($\text{R} = \text{Me, Et}$; **1** and **2** respectively) [4,5], can act as highly reducing, yet air-stable, reductants, capable of n-doping electron-transport materials relevant to organic electronics, including even compounds with relatively low-electron affinities such as copper phthalocyanine and 6,13-bis(tri(isopropyl)silylethynyl)pentacene [5–9]. These dimers are synthesized by electrochemical or alkali-metal one-electron reduction of the corresponding monomeric 18-electron cations. However, this reaction is by no means general; for example, while the above-mentioned iron and ruthenium species form dimers, $\text{Fe}(\eta^5\text{-C}_5\text{R}_5)(\eta^6\text{-C}_6\text{R}'_6)$ ($\text{R} = \text{H, Me}$; $\text{R}' = \text{Me, Et}$) are stable (in the absence of air) as neutral 19-electron monomers [3,10], and one-electron reduction of $[\text{Ru}(\eta^5\text{-C}_5\text{R}_5)(\eta^6\text{-C}_6\text{H}_6)]^+$ ($\text{R} = \text{H, Me}$) leads to formation of the 18-electron monomeric $\text{Ru}(\eta^5\text{-C}_5\text{R}_5)(\eta^5\text{-C}_6\text{H}_7)$ rather than to dimerization [4]. In an effort to develop new dimeric

doopants of this general class we synthesized hexafluorophosphate salts of the new 18-electron cations $[\text{RuCp}^*(\eta^6\text{-1,3,5-C}_6\text{H}_3(\text{CH}_2\text{SiMe}_3)_3)]^+$, **3**⁺, and $[\text{RuCp}^*(\eta^6\text{-C}_6\text{HMe}_5)]^+$, **4**⁺. Here we report their synthesis and crystal structures, along with that of $[\text{RuCp}^*(\eta^6\text{-1,3,5-C}_6\text{H}_3\text{Et}_3)]^+\text{PF}_6^-$, **2**⁺ PF_6^- . We also compare the electrochemistry and alkali-metal reductions of **2**⁺–**4**⁺ and $[\text{RuCp}^*(\eta^6\text{-1,3,5-C}_6\text{H}_3\text{Me}_3)]^+$, **1**⁺.

2. Experimental section

2.1. General details

All operations were performed under an atmosphere of nitrogen, either using standard Schlenk techniques or in a glove box. Tetrahydrofuran (THF) was distilled from sodium benzophenone, while toluene was dried over CaH_2 . Benzene-*d*₆ was dried over Na–K and stored in the glove box. $[\text{RuCp}^*(\text{NCMe})_3]^+\text{PF}_6^-$ [11], $[\text{RuCp}^*(\eta^6\text{-1,3,5-C}_6\text{H}_3\text{Me}_3)]^+\text{PF}_6^-$, **1**⁺ PF_6^- [12], $[\text{RuCp}^*(\eta^6\text{-1,3,5-C}_6\text{H}_3\text{Et}_3)]^+\text{PF}_6^-$, **2**⁺ PF_6^- [5], $[\text{FeCp}^*(\eta^6\text{-C}_6\text{H}_6)]^+\text{PF}_6^-$ [3], and $[\text{FeCp}^*(\eta^6\text{-1,3,5-C}_6\text{H}_3\text{Me}_3)]^+\text{PF}_6^-$ [13] were synthesized as previously described. All other reagents were purchased from Alfa-Aesar and used without further purification. ¹H and ¹³C{¹H} NMR

* Corresponding authors.

E-mail address: stephen.barlow@chemistry.gatech.edu (S. Barlow).

spectra were recorded on a Bruker AMX 400 MHz spectrometer. ^1H and ^{13}C chemical shifts were referenced to tetramethylsilane using the residual proton signal of the solvent and the carbon resonances of the deuterated solvent, respectively. Unless stated otherwise, carbon signals were observed as singlets. CHN analyses were carried out by Atlantic Microlabs (Norcross, GA) using a LECO 932 CHNS elemental analyzer, while the alkali metal content of $\text{K}^+\text{3}^-$ was determined by ALS Environmental (Tucson, AZ) using ICP-AES. Mass spectra were measured on an Applied Biosystems 4700 Proteomics Analyzer. The electrochemical data were acquired using cyclic voltammetry in 0.1 M $^n\text{Bu}_4\text{NPF}_6$ in dry THF under nitrogen, using a CH Instruments 620D potentiostat, a glassy carbon working electrode, a platinum wire auxiliary electrode, and, as a pseudo-reference electrode, a silver wire anodized in 1 M aqueous potassium chloride solution, at a scan rate of 50 mV s^{-1} . Ferrocene was used as an internal reference.

2.2. Synthesis of 1,3,5-tris(trimethylsilylmethyl)benzene

This compound was obtained by a modification of a literature procedure [14]. $^n\text{BuLi}$ (75 mL of a 2.87 M solution in hexanes, 215 mmol) and TMEDA (16 mL, 110 mmol) were stirred together at room temperature for 10 min and then added dropwise to mesitylene (5 mL, 35 mmol) cooled to $-78\text{ }^\circ\text{C}$. After 1 h at $-78\text{ }^\circ\text{C}$, the reaction vessel was brought slowly to room temperature, stirred for another 24 h, and cooled again to $-78\text{ }^\circ\text{C}$; chlorotrimethylsilane (22.8 mL, 180 mmol) was then added dropwise (CAUTION: vigorous reaction takes place) via a dropping funnel. The reaction mixture was stirred at room temperature overnight and filtered through Celite; the residue was washed with hexane and the washings were combined with the filtrate. This combined filtrate was washed with 5% aq. NaHCO_3 , then 5% aq. HCl , and finally with 5% aq. NaHCO_3 again. The organic layer was dried over Na_2SO_4 . The volatiles were removed by rotary evaporation and the resulting light yellow liquid was fractionally distilled ($175\text{--}180\text{ }^\circ\text{C}$, 0.07 mbar) to give the product (2.50 g, 21%). ^1H NMR (400 MHz, chloroform- d): δ 6.38 (s, 3H, arene CH), 1.97 (s, 6H, CH_2), 0.00 (s, 27H, TMS CH_3). $^{13}\text{C}\{^1\text{H}\}$ NMR (100 MHz, chloroform- d): δ 139.9 (arene quat.), 123.7 (arene CH), 26.8 (CH_2), -1.6 (TMS CH_3).

2.3. Synthesis of $\text{3}^+\text{PF}_6^-$

Freshly prepared $[\text{RuCp}^*(\text{NCMe})_3]^+\text{PF}_6^-$ (2.00 g, 3.96 mmol) was added to a thoroughly N_2 -deoxygenated solution of 1,3,5-tris(trimethylsilylmethyl)benzene (2.80 g, 8.5 mmol) and 1,2-dichloroethane (25 mL). The mixture was stirred for 12 h at room temperature and then at reflux for another 12 h. Evaporation of the solvent yielded a brown oily residue, which was extracted with acetone. The extracts were passed through a neutral alumina column, removing some brown material, and then evaporated to give a light yellow solid, which was recrystallized from dichloromethane and diethyl ether to give an off-white crystalline solid (1.44 g, 50%). ^1H NMR (400 MHz, acetone- d_6): δ 5.5 (s, arene CH, 3H), 1.90 (s, CH_2 , 6H), 1.87 (s, Cp^* , 15H), 0.07 (s, TMS, 27H). $^{13}\text{C}\{^1\text{H}\}$ NMR (100 MHz, acetone- d_6): δ 105.6 (arene quat.), 94.6 (Cp^* quat.), 85.9 (arene CH), 23.5 (CH_2), 9.8 (Cp^* CH_3), -1.6 (TMS CH_3). Anal. calcd for $\text{C}_{28}\text{H}_{51}\text{F}_6\text{PRuSi}_3$: C 46.84, H 7.15. Found: 45.96, H 6.86. ESI-MS: m/z 573 (cation M^+).

2.4. Synthesis of $\text{4}^+\text{PF}_6^-$

$\text{4}^+\text{PF}_6^-$ was obtained as a white crystalline solid (1.26 g, 50%) in an analogous fashion to $\text{3}^+\text{PF}_6^-$ from $[\text{RuCp}^*(\text{NCMe})_3]^+\text{PF}_6^-$ (2.40 g, 4.8 mmol) and 1,2,3,4,5-pentamethylbenzene (5.00 g, 33.7 mmol) in dichloroethane (20 mL). ^1H NMR (acetone- d_6): δ 5.81

(s, 1H, arene CH), 2.18 (s, 6H, arene CH_3), 2.15 (s, 3H, arene 3- CH_3), 2.12 (s, 6H, arene CH_3), 1.78 (s, 15H, Cp^* CH_3). $^{13}\text{C}\{^1\text{H}\}$ NMR (100 MHz, acetone- d_6): δ 99.8 (arene quat.), 99.7 (arene quat.), 99.4 (arene quat.), 93.5 (Cp^* quat.), 91.9 (arene CH), 17.7 (arene CH_3), 14.5 (arene CH_3), 14.0 (arene CH_3), 9.1 (Cp^* CH_3). Anal. calcd for $\text{C}_{21}\text{H}_{31}\text{F}_6\text{PRu}$: C 47.63, H 5.90. Found: C 47.77, H 6.04. ESI-MS: m/z 385 (cation M^+).

2.5. Synthesis of $\text{K}^+\text{3}^-$

Na-K alloy (3:1, 0.50 g, CAUTION, pyrophoric in air) was added to a solution of $\text{3}^+\text{PF}_6^-$ (0.47 g, 0.65 mmol) in THF; the reaction was stirred for 1 h at room temperature, after which time the THF solution was decanted off and evaporated under reduced pressure. The crude solid was extracted in toluene, filtered through Celite, and evaporated to give a red-orange solid, which was washed with cold pentane (3 mL) and dried under high vacuum (0.18 g, 0.29 mmol, 45%; CAUTION, pyrophoric in air). ^1H NMR (400 MHz, benzene- d_6): δ 4.54 (s, 1H, H_b), 4.33 (s, 1H, H_c), 2.46 (d, $J_{\text{H-H}} = 13.6\text{ Hz}$, 1H, H_g), 1.86 (s, 15H, Cp^*), 1.36 (m, 3H, overlap of H_a , H_d , H_f), 1.09 (d, $J_{\text{H-H}} = 16\text{ Hz}$, 1H, H_e), 0.80 (m, 2H, H_h), 0.38 (s, 9H, H_j), 0.31 (s, 9H, H_k), 0.05 (s, 9H, H_i). $^{13}\text{C}\{^1\text{H}\}$ NMR (100 MHz, benzene- d_6): δ 143.9 (arene quat. C_l), 126.4 (arene CH, C_c), 83.5 (arene quat. C_m), 79.9 (Cp^* quat.), 77.9 (arene CH, C_b), 55.6 (arene CH, C_a), 53.2 (arene quat., C_n), 28.8 (CH_2 , C_h), 25.3 (CH_2 , C_f), 23.5 (CH_2 , CH_{de}), 12.5 (Cp^* CH_3), 0.7 (TMS $_k$), -0.1 (TMS $_i$), -0.5 (TMS $_j$). Alkali metal analysis for $\text{C}_{28}\text{H}_{51}\text{KRuSi}_3$: K 6.39. Found: K 6.03 (Na < 0.9%). The resonances were mostly assigned using HSQC and NOE experiments; the quaternary ^{13}C arene resonances, however, were assigned on the basis of chemical shifts with reference to values reported for other η^4 -arenes in the literature and to the arene CH assignments. The labels used in the assignment of ^1H and ^{13}C resonances are shown below in Fig. 6.

2.6. Single crystal X-ray structure determinations

Crystallographic data and important refinement parameters for crystals of the hexafluorophosphates of 2^+ , 3^+ , and 4^+ are presented in Table 1. The X-ray diffraction experiments were carried out with a Bruker Apex II CCD area detector diffractometer, using graphite-monochromated Mo K_α radiation ($\lambda = 0.71073\text{ \AA}$) at 100(2) K. Absorption corrections were applied semi-empirically using the

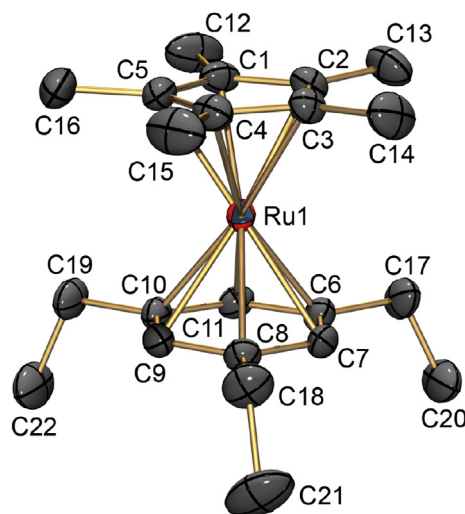


Fig. 1. ORTEP view (50% ellipsoids) of the cation in the crystal structure of $\text{2}^+\text{PF}_6^-$. Hydrogen atoms and counter ions are omitted for clarity.

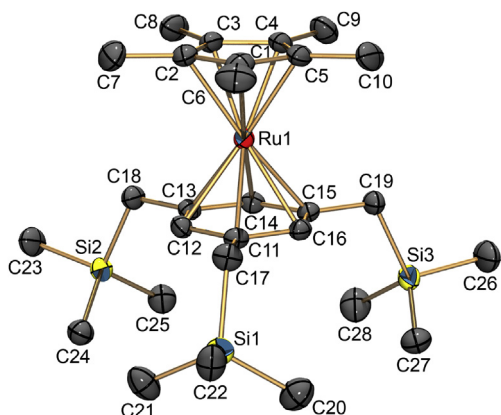


Fig. 2. ORTEP view (50% ellipsoids) of the cation in the crystal structure of $3^+PF_6^-$. Hydrogen atoms and counter ions are omitted for clarity.

APEX2 program [15]. The structures were solved by direct methods and refined by the full-matrix least-squares against F^2 in an anisotropic (for non-hydrogen atoms) approximation. All hydrogen atom positions were refined in an isotropic approximation using a “riding” model with the $U_{iso}(H)$ parameters equal to $1.2 U_{eq}(C_i)$, or, for methyl groups, equal to $1.5 U_{eq}(C_{ii})$, where $U(C_i)$ and $U(C_{ii})$ are respectively the equivalent thermal parameters of the carbon atoms to which the corresponding H atoms are bonded. The asymmetric unit of $2^+PF_6^-$ contains one complete cation and two half anions, with the phosphorus atoms of the anions, P1 and P2, located on inversion centers. The asymmetric units of $3^+PF_6^-$ and $4^+PF_6^-$ consist of a complete cation and a complete anion, but in the latter structure the anion is disordered, with two orientations of the anion present with occupancies of 0.66 and 0.34. All calculations were performed using the SHELXTL software [16].

3. Results and discussion

3.1. Synthesis

The dimer **1₂** has previously been reported by Gusev and co-workers [4], and we have previously reported **2₂**, which we synthesized in order to obtain a more soluble analog of **1₂** for solution doping studies and for mechanistic crossover experiments with **1₂** [5]. As we have discussed elsewhere, the reducing strength of these

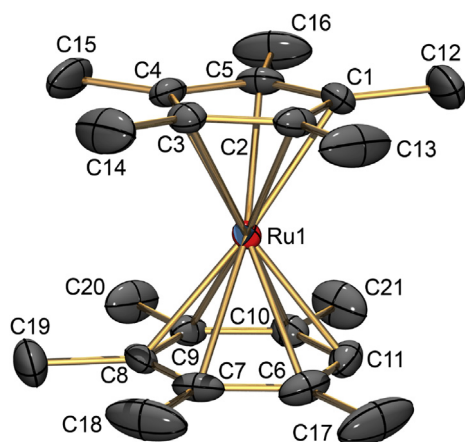


Fig. 3. ORTEP view (50% ellipsoids) of the cation in the crystal structure of $4^+PF_6^-$. Hydrogen atoms and counter ions are omitted for clarity.

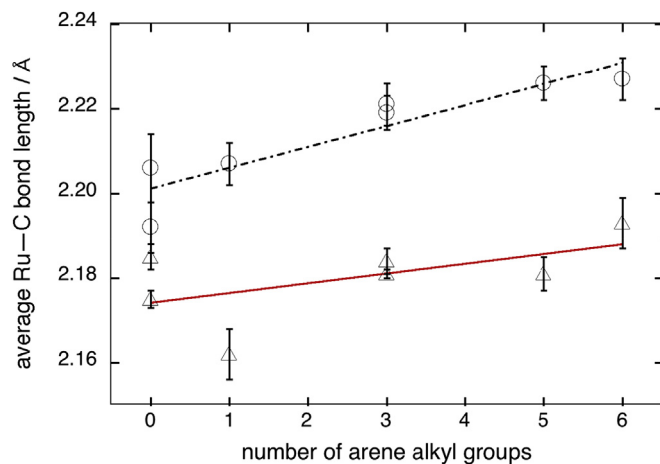


Fig. 4. Variation of average Ru–C_{arene} (circles) and Ru–C_{Cp*} (triangles) bond lengths (r) in crystal structures of $RuCp^*(\eta^6\text{-arene})$ salts with the number of arene alkyl substituents (n). Error bars are the estimated standard deviations for the average bond lengths. The lines are least-squares fits to the data and are described by the equations $r(\text{Ru–C}_{\text{arene}}) = 0.00495n + 2.201 \text{ \AA}$ and $r(\text{Ru–C}_{\text{Cp}^*}) = 0.00230n + 2.174 \text{ \AA}$.

dimers can be potentially increased by either a cathodic shift of the reduction potential of the corresponding monomeric 18-electron cation or by a weakening of the central C–C bond of the dimer [5,7]. Additional alkyl groups or more strongly electron-donating substituents might, therefore, afford more strongly reducing systems. However, as noted in the introduction, not all $RuCp^*(\text{arene})$ complexes dimerize when formed by reduction of the corresponding $[RuCp^*(\text{arene})]^+$ cations; in many cases, including that where arene = C_6Me_6 , hydrogen-atom abstraction to give species of the form $RuCp^*(\eta^5\text{-areneH})$ is preferred. In the case of **3**, trimethylsilylmethyl substituents were chosen since they are known to be significantly more electron-donating than simple alkyl substituents (for example, values of the Hammett coefficient, σ_p , of 0.00, -0.17 , and -0.21 have been obtained for H, Me, and CH_2SiMe_3 substituents, respectively [17]) and so would be expected to cathodically shift the $RuCp^*(\text{arene})^{+/0}$ potential, whereas the greater bulk of the substituents might be expected to contribute to a weaker C–C bond in the dimer than that in **1₂**. We were also interested in whether a dimer could be formed following reduction

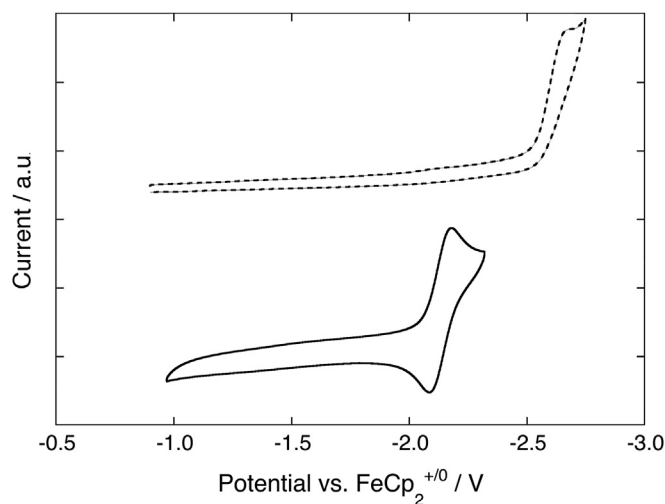


Fig. 5. Reductive cyclic voltammograms of $1^+PF_6^-$ (top, broken line) and its iron analogue, $[FeCp^*(\eta^6\text{-1,3,5-C}_6\text{H}_3\text{Me}_3)]^+PF_6^-$ (bottom, solid line), recorded in THF/0.1 M $n\text{-Bu}_4\text{N}^+PF_6^-$ at a scan rate of 50 mV s^{-1} .

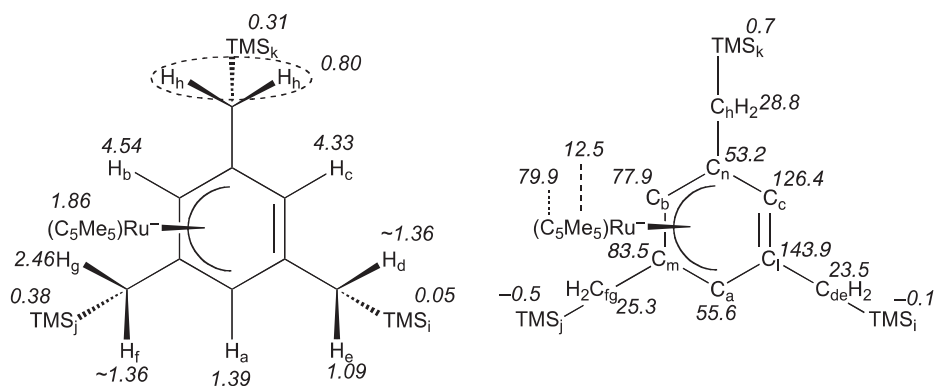


Fig. 6. Assignment of ^1H (left) and ^{13}C (right) NMR resonances for $\text{K}^+\mathbf{3}^+$ showing chemical shifts in ppm (see experimental section).

of $\text{RuCp}^*(\text{C}_6\text{Me}_5\text{H})^+$, $\mathbf{4}^+$, and whether the additional methyl groups would lead to a more reducing dimer than $\mathbf{1}_2$.

Both $\mathbf{3}^+\text{PF}_6^-$ and $\mathbf{4}^+\text{PF}_6^-$ were obtained in good yield as more-or-less colorless crystalline solids from the reaction of an excess of the appropriate arene with $[\text{RuCp}^*(\text{NCMe})_3]^+\text{PF}_6^-$ [11] in dichloroethane, in close analogy to the previously reported syntheses of $\mathbf{1}^+\text{PF}_6^-$ and $\mathbf{2}^+\text{PF}_6^-$ (Scheme 1) [5,12]. The sandwich compounds were fully characterized by ^1H and ^{13}C NMR spectroscopy, elemental analysis, and electrospray mass spectrometry. In the case of $\mathbf{3}^+$, the arene ligand was not commercially available, but was obtained by a modification of a literature procedure [14] in which mesitylene is deprotonated by a large excess of *n*-butyllithium/*N,N,N',N'*-tetramethylethylenediamine and the resulting trianion is quenched with chlorotrimethylsilane.

3.2. Molecular structure

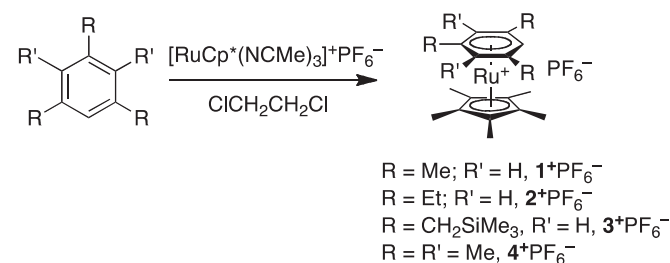
Single crystals of $\mathbf{2}^+\text{PF}_6^-$, $\mathbf{3}^+\text{PF}_6^-$, and $\mathbf{4}^+\text{PF}_6^-$ suitable for single crystal X-ray structure determination were obtained by slow evaporation of acetone solutions at room temperature. ORTEP representations of the cations in the structures are shown in Figs. 1–3, cell parameters and details of the data collection, solution, and refinement are given in Table 1, while selected bond lengths and angles are given in Table 2, along with comparative data for some other structures of $[\text{RuCp}^*(\eta^6\text{-arene})]^+$ salts from the literature [18–20]. In the structures of the $\mathbf{2}^+$ and $\mathbf{3}^+$ cations, the terminal methyl and SiMe_3 groups, respectively, of the arene substituents are bent away from the metal, thus meaning that the bulky substituents in the latter cation have little effect on the coordination geometry around the metal. The cations in all three structures have approximate axial symmetry, having essentially parallel Cp^* and arene rings (the dihedral angles are 1.06° , 0.66° , and 0.76° , for $\mathbf{2}^+\text{PF}_6^-$, $\mathbf{3}^+\text{PF}_6^-$, and $\mathbf{4}^+\text{PF}_6^-$, respectively) and centroid–metal–centroid angles very close to 180° , consistent with what is seen for other ruthenium cyclopentadienyl arene cation structures in the literature [18–24]. Ru–C bond distances are similar to those seen in related structures, with the Ru– C_{Cp^*} bonds being shorter than the Ru– C_{arene} bonds. Interestingly, as shown in Fig. 4, arene alkylation among the structures summarized in Table 2 appears to be correlated with a slight increase of the average Ru– C_{arene} bond length (variation of 0.035 \AA) and, to a lesser extent, of the average Ru– C_{Cp^*} distance (variation of 0.018 \AA) [25].

3.3. Electrochemistry

The potentials at which the Ru^{II} compounds $\mathbf{1}^+–\mathbf{4}^+$ are reduced to the corresponding 19-electron neutral Ru^{I} compounds $\mathbf{1}–\mathbf{4}$ were measured using cyclic voltammetry in $\text{THF}/^n\text{Bu}_4\text{N}^+\text{PF}_6^-$. All four compounds show qualitatively similar voltammograms, a representative example of which is shown in Fig. 5. As previously

Table 1
Crystal and structural refinement data.

	$\mathbf{2}^+\text{PF}_6^-$	$\mathbf{3}^+\text{PF}_6^-$	$\mathbf{4}^+\text{PF}_6^-$
Empirical formula	$\text{C}_{22}\text{H}_{33}\text{F}_6\text{PRu}$	$\text{C}_{28}\text{H}_{51}\text{F}_6\text{PRuSi}_3$	$\text{C}_{21}\text{H}_{31}\text{F}_6\text{PRu}$
fw	543.52	718.00	529.50
Cryst color, habit	Colorless prism	Colorless prism	Colorless prism
Crystal size, mm	$0.34 \times 0.29 \times 0.17$	$0.39 \times 0.35 \times 0.18$	$0.39 \times 0.36 \times 0.23$
Cryst syst	Monoclinic	Monoclinic	Monoclinic
Space group	$P2_1/c$	$P2_1/n$	$P2_1/n$
<i>a</i> , Å	17.8785(15)	10.9578(6)	9.1215(4)
<i>b</i> , Å	9.0536(8)	17.0020(10)	17.9170(8)
<i>c</i> , Å	15.3516(13)	18.9233(11)	13.8564(6)
β , deg	105.744(2)	92.9430(10)	104.5580(10)
<i>V</i> , Å ³	2391.7(4)	3520.8(3)	2191.84(17)
<i>Z</i>	4	4	4
ρ_{calc} , g cm ⁻³	1.509	1.355	1.605
μ (Mo <i>K</i> α), mm ⁻¹	0.775	0.641	0.843
<i>F</i> (000)	1112	1496	1080
θ Range, deg	2.37–28.00	2.10–28.00	1.90–28.00
Index ranges	$-23 \leq h \leq 23$ $-11 \leq k \leq 11$ $-20 \leq l \leq 20$	$-14 \leq h \leq 14$ $-22 \leq k \leq 22$ $-24 \leq l \leq 24$	$-12 \leq h \leq 12$ $-23 \leq k \leq 23$ $-18 \leq l \leq 18$
No. of reflns collected	26,200	39,149	24,497
No. of indep reflns	5774 ($R_{\text{int}} = 0.0353$)	8507 ($R_{\text{int}} = 0.0437$)	5291 ($R_{\text{int}} = 0.0336$)
No. of data/restraints/params	4897/0/282	6818/0/366	4448/15/278
GOF (F^2)	1.035	1.008	1.037
R_1 [$F > 2\sigma(F)$]	0.0362	0.0323	0.0453
wR_2 (F^2)	0.1000	0.0855	0.1309
(all data)			
Peaks min/max $e \text{ \AA}^{-3}$	0.817/–0.693	0.572/–0.397	1.153/–1.260



Scheme 1.

Table 2
Comparison of key geometric characteristics (Å, °) of RuCp*(η⁶-arene) salts.

Arene, anion	Ru–Cp [*]		Ru–C _{arene}		Ru–Ct _{Cp[*]} ^a	Ru–Ct _{arene^a}	Ct _{Cp[*]} –Ru–Ct _{arene}
	Range	Average	Range	Average			
C ₆ H ₆ , [RuCp*Br ₃] [–] [18]	2.170 (5)–2.182 (5)	2.175 (2)	2.181 (6)–2.208 (6)	2.192 (6)	1.811	1.711	177.8
C ₆ H ₆ , [RhCp*Cl ₃] [–] [19]	2.180 (5)–2.192 (5)	2.185 (3)	2.192 (6)–2.219 (5)	2.206 (8)	1.810	1.703	178.4
C ₆ H ₅ Me, [RuCp*Cl ₃] [–] [24]	2.148 (8)–2.179 (8)	2.162 (6)	2.181 (8)–2.219 (9)	2.207 (5)	1.794	1.714	178.9
C ₆ H ₃ Et ₃ (2 ⁺), PF ₆ [–]	2.177 (4)–2.194 (3)	2.184 (3)	2.210 (3)–2.235 (3)	2.219 (4)	1.813 (1)	1.708 (1)	179.44 (6)
C ₆ H ₃ (CH ₂ SiMe ₃) ₃ (3 ⁺), PF ₆ [–]	2.179 (2)–2.185 (2)	2.181 (1)	2.209 (2)–2.241 (2)	2.221 (5)	1.811 (1)	1.709 (1)	179.52 (4)
C ₆ HMe ₅ (4 ⁺), PF ₆ [–]	2.169 (4)–2.192 (4)	2.181 (4)	2.214 (3)–2.245 (4)	2.226 (4)	1.811 (1)	1.719 (1)	179.36 (8)
C ₆ Me ₆ , TCNQ [–] [20,21]	2.180 (2)–2.22 (2)	2.193 (6)	2.211 (6)–2.250 (7)	2.227 (5)	1.80	1.753	178.8

^a Ct denotes the centroid of the ring.

reported for other [RuCp(arene)]⁺ and [RuCp*(arene)]⁺ arene derivatives [4,26] and many other 18-electron sandwich complexes of the 4d- and 5d-metals [2,27–29], these are not reversible (with no observable reoxidation peak), consistent with the expected chemical reactivity of the 19-electron complexes. As shown in Table 3, replacement of the methyl substituents of 1⁺ by ethyl groups in 2⁺ lead to only a very small cathodic shift in the peak reduction potential, *E*_{pc}, whereas the CH₂SiMe₃ groups of 3⁺ lead to a cathodic shift of almost 0.3 V, consistent with Hammett coefficients, $\sigma_p(\text{Me}) \sim \sigma_p(\text{Et}) > \sigma_p(\text{CH}_2\text{SiMe}_3)$ [17]. The small cathodic shift of ca. 0.1 V seen on addition of two methyl groups to 1⁺ to give 4⁺ is similar to the difference seen between the peak reduction potentials of 1⁺ and [RuCp*(η⁶-C₆Me₆)]⁺ in acetonitrile [4].

Table 3 and Fig. 5 also shows that the reduction potential of 1⁺ is substantially cathodically shifted relative to that of its iron analog, [FeCp*(η⁶-1,3,5-C₆H₃Me₃)]⁺, consistent with the literature for other group 8 mixed-ring cations (for example, potentials previously reported for [MCp*(η⁶-C₆H₆)]⁺ {M = Fe, Ru} in acetonitrile [4,30]) and with the general tendency for the heavier transition elements to prefer higher oxidation states more strongly than their lighter congeners. Moreover, the electrochemistry of the iron compounds is considerably more reversible (*I*_{ox}/*I*_{red} = 1.0), indicating that the reduced iron species are all clearly less reactive than their ruthenium analogs. This is consistent with the greater tendency of the heavy transition metals to comply with the 18-electron rule, specifically with the fact that some iron species, such as FeCp*(η⁶-C₆Me₆), are stable as monomers, and that the dimerization of others, such as FeCp*(η⁶-C₆H₆), is sufficiently

slow that the 19-electron monomer can be observed in solution [31], whereas ruthenium examples rapidly give either dimers (e.g., 1₂) and/or hydrogen atom abstraction products (e.g., RuCp*(η⁵-C₆H₇)) [4].

3.4. Chemical reduction

As noted above, Gusev et al. have previously reported the chemical and electrochemical reduction reactions of a variety of cyclopentadienyl arene ruthenium cationic complexes [4,26]; depending on the substituents in question and the reduction conditions, a variety of products can be formed including dimers, hydrogen-reduced species, and, in some case, ligand redistribution products (for example, RuCp₂ is formed among the reduction products of [RuCp*(η⁶-C₆H₆)]⁺). Consistent with one of these reports [4], we found that Na/Hg reduction of 1⁺ gives the dimer 1₂ (Scheme 2), and that 2⁺ is reduced to an analogous dimer 2₂ under the same conditions [5]. We attempted the reduction of 4⁺PF₆[–] using Na/Hg in THF; MALDI mass spectra (*m/z* = 385, consistent with the monomer cation, as is seen in the MALDI spectra of 1₂ and 2₂) and elemental analysis are consistent with formation of a dimer, but NMR spectra were complicated, suggesting the possibility of an isomer mixture, perhaps accompanied by one or more isomers of a hydrogen reduction product.

While 1⁺, 2⁺, and 4⁺ can all be reduced using 1% Na amalgam, 3⁺PF₆[–] is largely unaffected by this reducing agent, at least on a

Table 3
Electrochemical potentials vs. ferrocenium/ferrocene for the reduction of 18-electron group 8 mixed-ring cations to the corresponding 19-electron species.

Cation	THF/0.1 M ⁿ Bu ₄ N ⁺ PF ₆ ^{–a}		MeCN/0.1 M ⁿ Bu ₄ N ⁺ BF ₄ ^{–c}	
	<i>E</i> _{1/2} /V	<i>E</i> _{pc} ^b	<i>E</i> _{1/2} /V ^d	<i>E</i> _{pc} /V ^e
[FeCp*(η ⁶ -C ₆ H ₆)] ⁺	–2.06	–	–2.07	–
[FeCp*(η ⁶ -1,3,5-C ₆ H ₃ Me ₃)] ⁺	–2.13	–	–	–
[RuCp*(η ⁶ -C ₆ H ₆)] ⁺	–	–	–	–2.72
[RuCp*(η ⁶ -1,3,5-C ₆ H ₃ Me ₃)] ⁺ , 1 ⁺	–	–2.67	–	–2.81
[RuCp*(η ⁶ -1,3,5-C ₆ H ₃ Et ₃)] ⁺ , 2 ⁺	–	–2.70	–	–
[RuCp*(η ⁶ -1,3,5-C ₆ H ₃ (CH ₂ SiMe ₃) ₃)] ⁺ , 3 ⁺	–	–2.96	–	–
[RuCp*(η ⁶ -C ₆ Me ₅ H)] ⁺ , 4 ⁺	–	–2.78	–	–
[RuCp*(η ⁶ -C ₆ Me ₆)] ⁺	–	–	–	–2.91

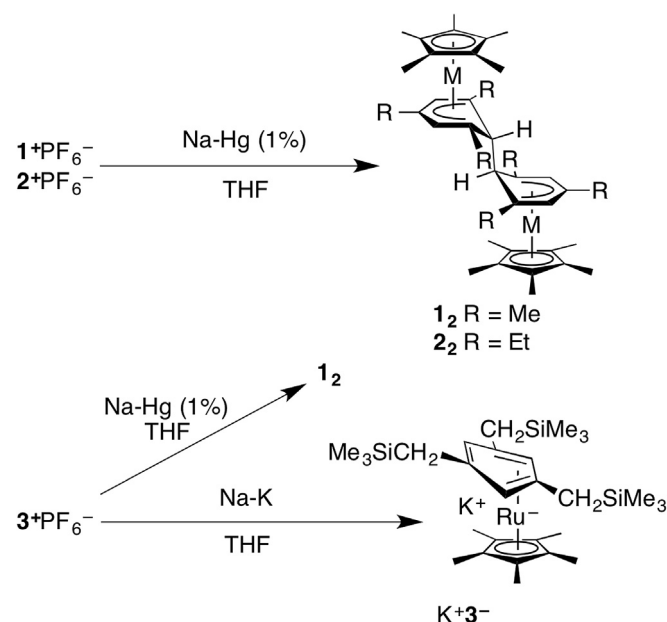
^a This work.

^b Peak potentials recorded at a scan rate of 50 mV s^{–1}.

^c Converted from data originally reported vs. SCE using a value of +0.40 V for FeCp₂^{+/0} vs. SCE in MeCN/0.1 M ⁿBu₄N⁺PF₆[–] taken from Ref. [32].

^d From Ref. [30].

^e Peak potentials at 100 mV s^{–1} from Ref. [4].



Scheme 2.

relatively short timescale (2 h), presumably due to the slightly more cathodic potential required for its reduction (see above). Evidently the reduction of $\text{RuCp}^*(\text{arene})$ cations with Na/Hg is of borderline feasibility. Indeed, the electrochemical potential for sodium amalgam has been estimated as ca. -2.2 to -2.4 V vs. $\text{FcPp}_2^{+/0}$ [32]. Longer reaction times still do not afford any direct reduction products of $\mathbf{3}^+$ and the majority of the material remains unchanged; however, ^1H and ^{13}C NMR spectroscopy indicated formation of the $\text{RuCp}^*(\text{mesitylene})$ dimer, $\mathbf{1}_2$, in 15–20% yield. Presumably the formation of $\mathbf{1}_2$ occurs by desilylation of $\mathbf{3}^+$ by either hydroxide (traces of which may have been introduced on the surface of the sodium) or fluoride (originating from PF_6^-), both of which are known to cleave Me_3Si –benzyl bonds [33–36], followed by reduction and dimerization of the more easily reduced $\mathbf{1}^+$ cation resulting from this cleavage. Use of a more powerful reducing agent – Na/K alloy – led to the formation of a benzene and toluene-soluble red-orange solid (in some cases accompanied by variable amounts of the desilylated dimer $\mathbf{1}_2$) that, in contrast to dimers such as $\mathbf{1}_2$ and $\mathbf{2}_2$, was pyrophoric in air, although the solid could be stored for several weeks without decomposition under inert atmosphere. The ^1H (^{13}C) NMR spectrum indicates that all three arene protons (CH carbon atoms), all three silyl groups, and all three benzyl methylene groups are inequivalent. Moreover, the protons of each methylene are noticeably diastereotopic; two of the CH_2 groups are seen as pairs of well-separated doublets (i.e., each constitutes an AX spin system), while another is observed as an AB multiplet. The protons of two of the arene CH groups and two of the CH_2 groups show strong inter-ring NOEs with the Cp^* protons, while a CH signal at 4.33 ppm and the protons of one of the CH_2 AX systems do not. These observations are consistent with the arene adopting an η^4 coordination mode. Additional NOE experiments allow all the proton resonances to be assigned, as shown in Fig. 6. The NOE experiments allow us to assign the nominally sp^2 CH group seen at the unusually high-field chemical shift of 1.39 ppm to the CH group at one end of the η^4 portion of the arene (labeled “a” in Fig. 6). Similarly upfield shifts have been reported for the corresponding resonances of other η^4 -arene complexes; for example, $\text{Os}(\eta^4\text{-C}_6\text{H}_6)(\eta^6\text{-C}_6\text{H}_6)$ (3.00 ppm) [37,38], $[\text{Cr}(\eta^4\text{-naph})(\text{CO})_3]^{2-}$ (2.00 ppm) [39], $[\text{Mn}(\eta^4\text{-naph})(\text{CO})_3]^-$ (2.44 ppm) [40], $\text{TaMe}(\eta^4\text{-naph})(\text{dmpe})_2$ (1.51 ppm) [41], and $\text{Fe}(\eta^4\text{-C}_6\text{H}_6)\text{tmps}$ (1.69 ppm) [42,43] {naph = naphthalene, dmpe = $\text{Me}_2\text{PCH}_2\text{CH}_2\text{PMe}_2$; tmps = $\text{MeSi}(\text{CH}_2\text{PMe}_2)_3$. The high-field shift is consistent with the expected distortion of the geometry of the C_a atom from planarity, as revealed in the crystal structures of various other η^4 -arene complexes. An HSQC experiment allows most of the ^{13}C resonances to be assigned; the C_a resonance is also seen at characteristically high field (55.6 ppm), similar to what is seen for $\text{Os}(\eta^4\text{-C}_6\text{H}_6)(\eta^6\text{-C}_6\text{H}_6)$ (47.2 ppm) [37,38], $[\text{Cr}(\eta^4\text{-naph})(\text{CO})_3]^{2-}$ (56.2 ppm) [39], $[\text{Mn}(\eta^4\text{-naph})(\text{CO})_3]^-$ (57.6 ppm) [40], and $\text{Fe}(\eta^4\text{-C}_6\text{H}_6)\text{tmps}$ (48.5 ppm) [42,43]. The η^4 -arene and the pyrophoric nature of the compound are consistent with the formation of an 18-electron Ru^0 anionic complex; ICP analytical results indicate that the counterion is potassium. Although alkali ions are often coordinated by donors such as ethers, the NMR spectra indicate that no THF is present in this compound.

Two-electron reduction processes are often accompanied by shifts from η^6 - to η^4 -arene coordination, enabling retention of an 18-electron configuration at the metal center; examples of systems that have been well-characterized crystallographically and/or by NMR include $[\text{Cr}(\text{naph})(\text{CO})_3]^{0/2-}$ [39], $[\text{Mn}(\text{C}_6\text{H}_6)(\text{CO})_3]^{+/-}$ [40], $[\text{Ru}(\text{arene})_2]^{2+/0}$ (which, as in the case of $\mathbf{3}^{+/-}$ are formally $\text{Ru}^{\text{II}/0}$ couples) [44–48], and $[\text{MCp}^*(\text{C}_6\text{Me}_6)]^{2+/0}$ {M = Rh, Ir} [49]. Although two one-electron reductions have been observed electrochemically for several $[\text{FeCp}(\text{arene})]^+$ species [50–52], we are unaware of the previous isolation of any anionic mixed

cyclopentadienyl/arene complexes of a group 8 metal. Moreover, $\text{FeCp}(\text{arene})$ anions are likely to be 20-electron η^6 -arene species [50,51], consistent with the general tendency for sandwich compounds of the 3d metals to retain axial symmetry, even when this leads to deviation from the 18-electron rule.

It is unclear to us exactly why $\mathbf{3}^-$ is isolated, rather than the corresponding dimer or hydrogen abstraction products [53]. It is worth noting that Na/K reduction of $\mathbf{1}^+$ and $\mathbf{2}^+$ still leads to the dimer, suggesting that formation of the two-electron reduction product is a not only a consequence of the stronger reducing agent. Perhaps the greater bulk of the substituents reduces the rate of these reactions sufficiently to allow time for a second electron to be transferred to $\mathbf{3}^+$ from the highly reducing Na/K.

4. Conclusion

The X-ray structures of three $[\text{RuCp}^*(\text{arene})]^+\text{PF}_6^-$ salts, where arene = 1,3,5-triethylbenzene, 1,3,5-tris(trimethylsilylmethyl)benzene, and 1,2,3,4,5-pentamethylbenzene, have been determined. Their electrochemical and chemical reduction has been examined. All three undergo one-electron reduction processes at highly cathodic potentials. Whereas reduction of the 1,3,5-triethylbenzene example gives an air-stable dimer, $(\text{Ru}^{\text{II}}\text{Cp}^*)_2(\mu\text{-}\eta^5\text{:}\eta^5\text{-C}_6\text{H}_3\text{Et}_3\text{C}_6\text{H}_3\text{Et}_3)$, analogous to that previously reported for the mesitylene derivative, Na/K reduction of $[\text{Ru}^{\text{II}}\text{Cp}^*\{\eta^6\text{-C}_6\text{H}_3(\text{CH}_2\text{SiMe}_3)_3\}]^+$ led to the formation of $\text{K}^+[\text{Ru}^0\text{Cp}^*\{\eta^4\text{-C}_6\text{H}_3(\text{CH}_2\text{SiMe}_3)_3\}]^-$, which was extensively characterized by NMR methods and represents the first example of a group 8 $[\text{MCp}(\text{arene})]^-$ derivative to be isolated.

Acknowledgments

We thank Solvay SA, the National Science Foundation (through the STC Program, DMR-0120967, and the PREM program, DMR-0934212), and the Office of Naval Research (N00014-11-1-0313) for support, Les Gelbaum for help with NMR measurements, and John Bacsa with his efforts to determine the structure of $\text{K}^+\mathbf{3}^-$ from poor quality crystals.

Appendix A. Supplementary material

CCDC 926155, 926156 and 926157 contain the supplementary crystallographic data for this paper. These data can be obtained free of charge from The Cambridge Crystallographic Data Centre via www.ccdc.cam.ac.uk/data_request/cif.

References

- [1] E.O. Fischer, H. Wawersik, *J. Organomet. Chem.* 5 (1966) 559.
- [2] N. El Murr, J.E. Sheats, W.E. Geiger, J.D.L. Holloway, *Inorg. Chem.* 18 (1979) 1443.
- [3] J.-R. Hamon, D. Astruc, P. Michaud, *J. Am. Chem. Soc.* 103 (1981) 758.
- [4] O.V. Gusev, M.A. Ievlev, M.G. Peterleitner, S.M. Peregudova, L.I. Denisovich, P.V. Petrovskii, N.A. Ustyniuk, *J. Organomet. Chem.* 534 (1997) 57.
- [5] S. Guo, S.B. Kim, S.K. Mohapatra, Y. Qi, T. Sajoto, A. Kahn, S.R. Marder, S. Barlow, *Adv. Mater.* 24 (2012) 699.
- [6] Y. Qi, S.K. Mohapatra, S.B. Kim, S. Barlow, S.R. Marder, A. Kahn, *Appl. Phys. Lett.* 100 (2012) 083305.
- [7] S. Guo, S.K. Mohapatra, A. Romanov, T.V. Timofeeva, K.I. Hardcastle, K. Yesudas, C. Risko, J.-L. Brédas, S.R. Marder, S. Barlow, *Chem. Eur. J.* 18 (2012) 14760.
- [8] S. Olthof, S. Mehraeen, S.K. Mohapatra, S. Barlow, V. Coropceanu, J.-L. Brédas, S.R. Marder, A. Kahn, *Phys. Rev. Lett.* 109 (2012) 176601.
- [9] S. Olthof, S. Singh, S.K. Mohapatra, S. Barlow, S.R. Marder, B. Kippelen, A. Kahn, *Appl. Phys. Lett.* 101 (2012) 253303.
- [10] D. Astruc, *New J. Chem.* 33 (2009) 1191.
- [11] B. Steinmetz, W.A. Schenk, *Organometallics* 18 (1999) 943.
- [12] J.L. Schrenk, A.M. McNair, F.B. McCormick, K.R. Mann, *Inorg. Chem.* 25 (1986) 3501.
- [13] J.-R. Hamon, J.-Y. Saillard, A. Le Beuze, M.J. McGlinchey, D. Astruc, *J. Am. Chem. Soc.* 104 (1982) 7549.
- [14] J. Klein, A. Medlik, A.Y. Meyer, *Tetrahedron* 32 (1976) 51.
- [15] Bruker, APEX2 Software Package, Bruker AXS Inc., Madison, WI, 2005.

- [16] G.M. Sheldrick, SHELXTL-NT v. 6.12, Structure Determination Software Suite, Bruker AXS Inc., Madison, WI, 2001.
- [17] C. Hansch, A. Leo, R.W. Taft, *Chem. Rev.* 91 (1991) 165.
- [18] C. Gemel, K. Mereiter, R. Schmid, K. Kirchner, *Organometallics* 15 (1996) 532.
- [19] L. Quebette, R. Scopelliti, K. Severin, *Eur. J. Inorg. Chem.* (2006) 231.
- [20] P.J. Fagan, M.D. Ward, J.C. Calabrese, *J. Am. Chem. Soc.* 111 (1989) 1698.
- [21] M.D. Ward, P.J. Fagan, J.C. Calabrese, D.C. Johnson, *J. Am. Chem. Soc.* 111 (1989) 1719.
- [22] H. Aneetha, M. Jiménez-Tenorio, M.C. Puerta, P. Valerga, V.N. Sapunov, R. Schmid, K. Kirchner, K. Mereiter, *Organometallics* 21 (2002) 5334.
- [23] S.P. Nolan, K.L. Martin, E.D. Stevens, *Organometallics* 11 (1992) 3947.
- [24] M.E. Navarro Clemente, P. Juárez Saavedra, M. Cervantes Vásquez, M.A. Paz-Sandoval, A.M. Arif, R.D. Ernst, *Organometallics* 21 (2002) 592.
- [25] While the detailed explanation of the trend seen in Fig. 4 is unclear to us at this point, alkylation is unlikely to have a significant steric effect in these systems, and so the observed trends might, therefore, be attributable to the inductive donor effects of the alkyl groups (although, as noted in the discussion of the electrochemical data, the different alkyl groups considered here have different donor strengths). Alkylation is expected to increase the σ and π donor (in pseudo-axial symmetry) strength and decrease the δ -acceptor strength of the arene. The observed trends are consistent with the variation in the δ -acceptor properties dominating the Ru–Carene bond lengths, and the donor properties, competing with the donor properties of the Cp* ligand, affecting the Ru–Cp* bond. However, this picture is apparently inconsistent with previous calorimetric studies have shown that alkylation results in overall stronger binding of the arene to the metal (ref [23]).
- [26] O.V. Gusev, M.A. Ievlev, T.A. Peganova, M.G. Peterleitner, P.V. Petrovskii, Y.F. Oprunenko, N.A. Ustynyuk, *J. Organomet. Chem.* 551 (1998) 93.
- [27] O.V. Gusev, M.G. Peterleitner, M.A. Ievlev, A.M. Kal'sin, P.V. Petrovskii, L.I. Denisovich, N.A. Ustynyuk, *J. Organomet. Chem.* 531 (1997) 95.
- [28] O.V. Gusev, L.I. Denisovich, M.G. Peterleitner, A.Z. Rubezhov, N.A. Ustynyuk, P.M. Maitlis, *J. Organomet. Chem.* 452 (1993) 219.
- [29] S.K. Mohapatra, A. Romanov, G. Angles, T.V. Timofeeva, S. Barlow, S.R. Marder, *J. Organomet. Chem.* 706–707 (2012) 140.
- [30] D. Astruc, *Chem. Rev.* 88 (1988) 1189.
- [31] D. Astruc, J.-R. Hamon, G. Althoff, E. Román, P. Batail, P. Michaud, J.-P. Mariot, F. Varret, D. Cozak, *J. Am. Chem. Soc.* 101 (1979) 5445.
- [32] N.G. Connelly, W.E. Geiger, *Chem. Rev.* 96 (1996) 877.
- [33] C.R. Hauser, C.R. Hance, *J. Am. Chem. Soc.* 73 (1951) 5846.
- [34] J. Chmielecka, J. Chojnowski, W.A. Stanczyk, C. Eaborn, *J. Chem. Soc. Perkin Trans. 2* (1989) 865.
- [35] C.H. DePuy, V.M. Bierbaum, L.A. Flippin, J.J. Grabowski, G.K. King, R.J. Schmitt, S.A. Sullivan, *J. Am. Chem. Soc.* 102 (1980) 5012.
- [36] G.G. Gatev, M. Zhong, J.I. Brauman, *J. Phys. Org. Chem.* 10 (1997) 531.
- [37] J.A. Bandy, M.L.H. Green, D. O'Hare, K. Prout, *J. Chem. Soc. Chem. Commun.* (1984) 1402.
- [38] J.A. Bandy, M.L.H. Green, D. O'Hare, *J. Chem. Soc. Dalton Trans.* (1986) 2477.
- [39] R.D. Rieke, W.P. Henry, J.S. Arney, *Inorg. Chem.* 26 (1987) 420.
- [40] R.L. Thompson, S. Lee, A.L. Rheingold, N.J. Cooper, *Organometallics* 10 (1991) 1657.
- [41] J.O. Albright, S. Datta, B. Dezube, J.K. Kouba, D.S. Marynick, S.S. Wreford, B.M. Foxman, *J. Am. Chem. Soc.* 101 (1979) 611.
- [42] J.M. Boncella, M.L.H. Green, D. O'Hare, *J. Chem. Soc. Chem. Commun.* (1986) 618.
- [43] J.M. Boncella, M.L.H. Green, *J. Organomet. Chem.* 325 (1987) 217.
- [44] E.O. Fischer, C. Elschenbroich, *Chem. Ber.* 103 (1970) 162.
- [45] G. Huttner, S. Lange, E.O. Fischer, *Angew. Chem. Int. Ed.* 10 (1971) 556.
- [46] R.G. Finke, R.H. Voegeli, E.D. Laganis, V. Boekelheide, *Organometallics* 2 (1983) 347.
- [47] R.H. Voegeli, H.C. Kang, R.G. Finke, V. Boekelheide, *J. Am. Chem. Soc.* 108 (1986) 7010.
- [48] R.L. Lord, C.K. Schauer, F.A. Schultz, M.-H. Baik, 133 (2011) 18234.
- [49] W.J. Bowyer, W.E. Geiger, *J. Am. Chem. Soc.* 107 (1985) 5657.
- [50] N. El Murr, *J. Chem. Soc. Chem. Commun.* (1981) 251.
- [51] A.S. Abd-El-Aziz, A.S. Baranski, A. Piórko, R.G. Sutherland, *Inorg. Chim. Acta* 147 (1988) 77.
- [52] A.S. Abd-El-Aziz, K. Winkler, A.S. Baranski, *Inorg. Chim. Acta* 194 (1992) 207.
- [53] Electrochemistry in THF, the solvent used for the chemical reduction, does not provide any useful insights as even the first reduction is very close to the solvent-breakdown potential